Ido *et al. Journal of Wood Science (2025) 71:53*
https://doi.org/10.1186/s10086-025-02228-7

Journal of Wood Science

ORIGINAL ARTICLE

Open Access

Evaluation of out-of-plane bending performance of cross-laminated timber (CLT) with various layups made from Japanese cedar (*Cryptomeria japonica*)

Hirofumi Ido[1*], Ryutaro Sudo[2], Kohta Miyamoto[1] and Atsushi Miyatake[1]

Abstract

This study assesses the out-of-plane bending performance of cross-laminated timber (CLT) panels made from Japanese cedar to determine the bending modulus of elasticity (*E*) and shear modulus (*G*) through both dynamic and static testing methods. Six CLT layups, as defined by the Japanese Agricultural Standard (JAS) 3079, were tested in both major and minor strength directions. The findings reveal that *E* values obtained from the Timoshenko–Goens–Hearmon (TGH) method, the variable span method, and the shear-free (local) values of the out-of-plane bending test were generally consistent. However, the values derived from the transformed section method were generally lower, especially in the minor strength direction. The TGH method consistently yielded higher *G* values compared to the variable span method, which exhibited irregular patterns in minor strength direction layups with fewer layers. The *E/G* ratios from the variable span method reached approximately 80 for certain layups in the major strength direction, surpassing the default value of 50 used in JAS 3079. This indicates the need for an adjustment factor near 0.85, rather than the default 0.9 specified in JAS 3079. While the 0.9 adjustment factor is appropriate for most CLT layups, it can underestimate deformation in those susceptible to rolling shear. In addition, out-of-plane bending test results show that the 0.65 reduction factor from the Notification of the Ministry of Land, Infrastructure, Transport and Tourism is suitable for the major strength direction but may be too conservative for layups in the minor strength direction.

Keywords Cross-laminated timber, Out-of-plane bending, Japanese cedar, Bending modulus of elasticity, Shear modulus

Introduction

Typical methods for analyzing the out-of-plane bending modulus of elasticity (*E*) of cross-laminated timber (CLT), as outlined in the CLT Handbook [1], include mechanically jointed beams theory, composite theory, and the shear analogy method. In addition, several other approaches have been investigated, particularly focusing on the effects of rolling shear under out-of-plane bending conditions [2–9].

In contrast, the Japanese Agricultural Standard for Cross Laminated Timber (JAS 3079) [10] uses the transformed section method (E_{TS}) [11] to determine the out-of-plane apparent bending modulus of elasticity (E_{app}) and bending strength of CLT. According to JAS 3079 [10], each lamina's bending modulus is considered the true bending modulus of elasticity (E_{true}), and the overall true bending modulus of the CLT is calculated based on this [12]. This true modulus is then

*Correspondence:
Hirofumi Ido
ido_hirofumi650@ffpri.go.jp
[1] Forestry and Forest Products Research Institute, 1 Matsunosato, Tsukuba, Ibaraki 305-8687, Japan
[2] Graduate School of Environmental, Life, Natural Science and Technology, Okayama University, Okayama 700-8530, Japan

© The Author(s) 2025, corrected publication 2025. **Open Access** This article is licensed under a Creative Commons Attribution 4.0 International License, which permits use, sharing, adaptation, distribution and reproduction in any medium or format, as long as you give appropriate credit to the original author(s) and the source, provide a link to the Creative Commons licence, and indicate if changes were made. The images or other third party material in this article are included in the article's Creative Commons licence, unless indicated otherwise in a credit line to the material. If material is not included in the article's Creative Commons licence and your intended use is not permitted by statutory regulation or exceeds the permitted use, you will need to obtain permission directly from the copyright holder. To view a copy of this licence, visit http://creativecommons.org/licenses/by/4.0/.

converted into the apparent bending modulus through a third-point bending test with a span-to-depth ratio of 21, as specified in JAS 3079 [10]. During this conversion, an adjustment factor of 0.9 is applied to the calculated true bending modulus to yield the E_{app} [12].

This adjustment factor of 0.9 is based on the assumptions that the span-to-depth ratio is 21 and the ratio of E_{true}/G (where G is the shear modulus) is equal to 50 [12]. However, when the E_{true}/G ratio exceeds 50 in actual bending behavior, the apparent bending modulus is lower than predicted by JAS 3079 [10], leading to greater deformation. A previous study that dynamically measured true bending modulus and G for several CLT layups found that the E_{true}/G ratio peaked at approximately 50 [13]. Still, this study did not cover all CLT layups specified in JAS 3079 [10], nor did it include static measurements of the E_{true}/G ratio.

In addition, while numerous studies have examined the bending performance of CLTs with outer laminae aligned parallel to the specimen's length (the major strength direction), relatively few have focused on configurations, where the outer laminae are oriented perpendicular to the length (the minor strength direction), with only a limited number of studies addressing this aspect [14–16].

Therefore, this study aimed to evaluate the modulus of elasticity and G of CLTs specified in JAS 3079 [10] using both dynamic and static testing methods. The tested layups included 9-layer 9-ply, 7-layer 7-ply, 5-layer 7-ply, 5-layer 5-ply, 3-layer 4-ply, and 3-layer 3-ply panels. All CLTs were Mx60 grade, with all laminae manufactured from Japanese cedar (*Cryptomeria japonica*).

The dynamic modulus of elasticity was determined using the TGH method, which estimates both the true bending modulus and G by analyzing multiple natural frequencies [17, 18]. In contrast, the static modulus of elasticity was measured using the variable span method, which derives the true bending modulus and G from deflection behavior at different span-to-depth ratios during a three-point bending test [19]. By comparing the results from these two methods, the study examined differences in the evaluated true bending and G values to understand how the testing method influenced the measured mechanical properties.

Finally, out-of-plane bending tests were performed in accordance with JAS 3079 [10] to determine the bending strength and assess the overall out-of-plane performance of the CLT specimens.

Materials and methods

Manufacture of CLT and lamina specimens

The cross sections of the manufactured CLT specimens and the grades of laminae used are presented in Fig. 1. All laminae were made from Japanese cedar, each measuring 30 mm × 122 mm in cross section. The outer layers consisted of M60B-grade laminae, with an E between 5.0 and 9.0 kN/mm^2, while the inner layers were composed of M30B-grade laminae, ranging from 2.5 to 6.0 kN/mm^2. The laminae were longitudinally finger-jointed using an aqueous polymer-isocyanate (API) adhesive. These joints

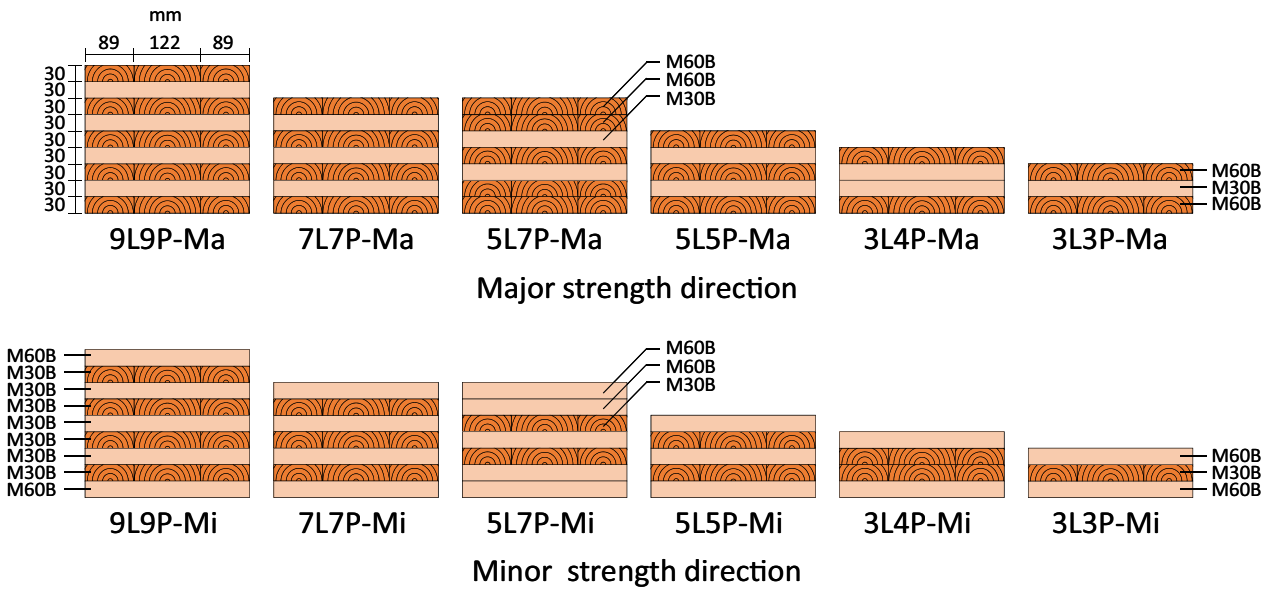


Fig. 1 Cross sections and grades of laminae used in each CLT specimen. The annual ring orientation in the laminae was arranged randomly in the actual specimens

were arranged horizontally, with finger profiles visible on the narrow faces of the laminae, and each finger joint had a length of 16 mm.

Motherboards for each layup configuration were fabricated using these laminae and laminated together with the API adhesive, leaving the side (narrow) surfaces of the laminae unglued. For each layup, two types of CLTs were produced: major strength direction CLTs, where the grain direction of the outer laminae aligned parallel to the specimen length, and minor strength direction CLTs, where the grain direction of the outer laminae was perpendicular to the specimen length. CLT specimens for each layup were cut from their respective motherboards, with all specimens from a given layup originating from a single motherboard. The specimen length was set to 23 times its depth to suit bending tests. All CLTs had a consistent width of 300 mm. The central lamina maintained its full width of 122 mm, while the laminae on either side were trimmed to achieve the overall specified width. Table 1 provides the detailed CLT dimensions and the number of specimens for each layup.

In addition to the CLT specimens, thirty M60B and thirty M30B lamina bending specimens were prepared, each measuring 1000 mm in length, 122 mm in width, and 30 mm in thickness, with a finger joint positioned at the center of the length. These specimens were used to analyze the bending behavior of the CLTs. All manufacturing processes were performed by Meiken Lamwood Corporation.

Measurement of modulus of elasticity and shear modulus by dynamic tests

The density of each CLT specimen was measured, and the modulus of elasticity in the longitudinal direction was determined using the longitudinal vibration method. During this test, each specimen was supported at points located 0.224 times its length from each end. A hammer strike was applied to one cross-sectional end to induce longitudinal vibrations, which were detected by an accelerometer (NP-3120, Ono Sokki Co., Ltd.) attached to the opposite end. The first resonant frequency was recorded using a fast Fourier transform (FFT) analyzer (CF-4500, Ono Sokki Co., Ltd.). Subsequently, out-of-plane flexural vibrations were dynamically measured. In this test, the support conditions for each specimen matched those used in the longitudinal vibration test. A hammer strike was applied to one end's top surface to induce flexural vibrations, detected by an accelerometer (NP-3120, Ono Sokki Co., Ltd.) positioned near the impact point. Resonant frequencies from the first to the seventh modes were recorded using an FFT analyzer (CF-4500, Ono Sokki Co., Ltd.). However, for the 3L3P-Mi specimens, the second-mode frequency was excluded from the analysis owing to unclear detection.

An example of the measurement setup for the 9L9P-Ma specimen is shown in Fig. 2. The E_{true} and G were calculated using the Timoshenko–Goens–Hearmon (TGH) flexural vibration method [17, 18], assuming a shear stress distribution coefficient of 1.2.

Measurement of bending modulus of elasticity and shear modulus by static tests

The E and G were determined using the variable span method [19]. Figure 3 shows the test setup for the 9L9P-Ma specimen. Each CLT specimen underwent three-point bending tests performed on a universal testing machine (SAH-100-SS, Maekawa Testing Machine Mfg Co., Ltd.). The span lengths were set at 21, 17, 12, and 7 times the specimen depth. To prevent initial deflection

Table 1 Dimensions and quantity of CLT specimens for each layup

Group	Layup	Strength direction	Depth (mm)	Width (mm)	Length (mm)	Number of specimens
9L9P-Ma	9-layer 9-ply	Major	270	300	6210	8
9L9P-Mi	9-layer 9-ply	Minor	270	300	6210	8
7L7P-Ma	7-layer 7-ply	Major	210	300	4830	8
7L7P-Mi	7-layer 7-ply	Minor	210	300	4830	8
5L7P-Ma	5-layer 7-ply	Major	210	300	4830	8
5L7P-Mi	5-layer 7-ply	Minor	210	300	4830	8
5L5P-Ma	5-layer 5-ply	Major	150	300	3450	6
5L5P-Mi	5-layer 5-ply	Minor	150	300	3450	6
3L4P-Ma	3-layer 4-ply	Major	120	300	2760	6
3L4P-Mi	3-layer 4-ply	Minor	120	300	2760	6
3L3P-Ma	3-layer 3-ply	Major	90	300	2070	12
3L3P-Mi	3-layer 3-ply	Minor	90	300	2070	12



Fig. 2 Dynamic test (TGH method) performed on the 9L9P-Ma specimen

when placing the specimen on the supports, a small preload was applied before starting the test.

The load applied to each specimen was calculated by multiplying the specified design strength of each CLT by a long-term performance factor of 1.1/3 [20]. To measure deflection during loading, a displacement transducer (CDP-50, Tokyo Measuring Instruments Laboratory Co., Ltd.) was brought into contact with an L-shaped bracket, which was attached to the mid-span and mid-depth of the specimen's side face.

The E_{app} for each span condition was determined from the load–deflection relationship. For each specimen, a graph was plotted with $(d/L)^2$ on the x-axis and $1/E_{app}$ on the y-axis, where d represents the specimen depth and L the span length. A regression line was then fitted to four data points using the least squares method. The E_{true} and G were derived from the intercept $a = 1/E_{true}$ and slope $b = 1.2/G$, respectively [19].

However, three out of eight 5L7P-Mi specimens and four out of twelve 3L3P-Mi specimens were excluded from the final analysis owing to their coefficient of determination (R^2) being below 0.9.

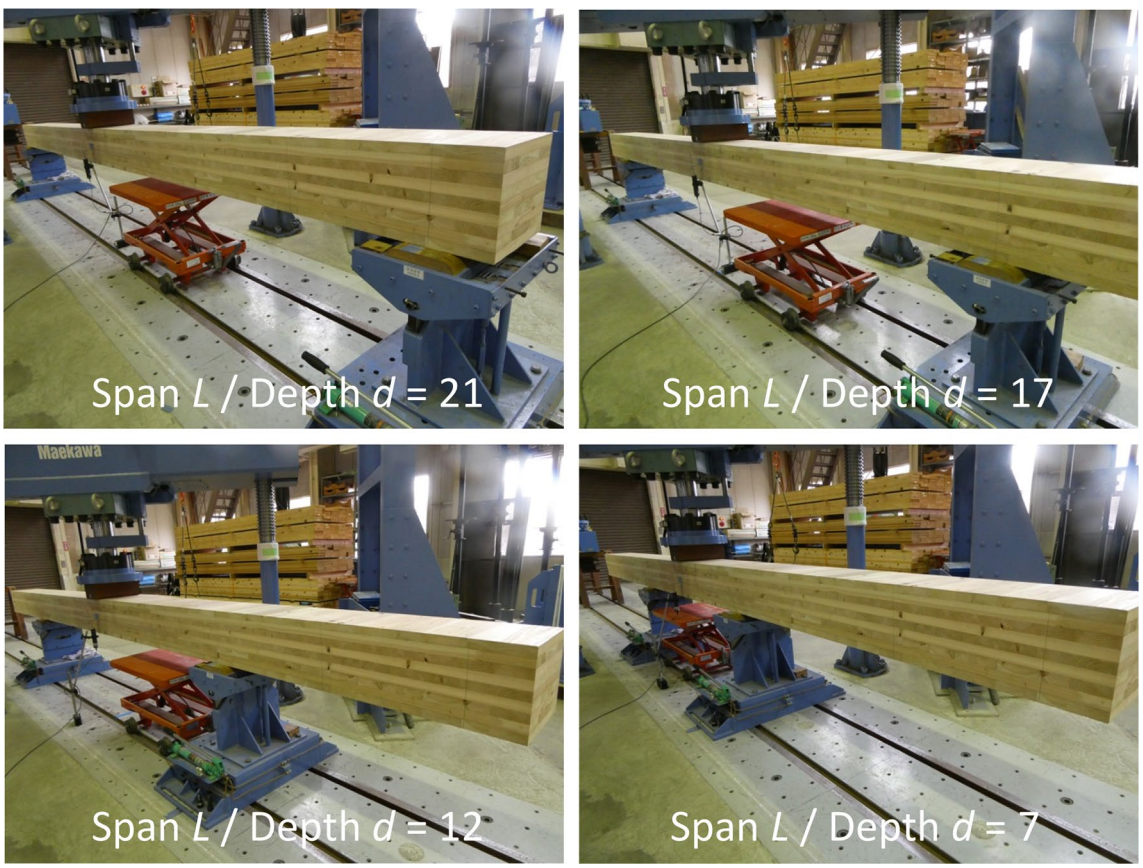


Fig. 3 Example of the test setup for the 9L9P-Ma specimen

Out-of-plane bending tests of CLT and lamina: dynamic and static methods

Out-of-plane bending tests were performed on the CLT specimens after the dynamic and static tests, in accordance with the bending test method outlined in JAS 3079 [10]. All specimens were tested except for six out of twelve specimens from both the 3L3P-Ma and 3L3P-Mi groups.

The tests used a third-point loading configuration, with a span length set at 21 times the specimen depth. A universal testing machine (SAH-100-SS, Maekawa Testing Machine Mfg Co., Ltd.) was used to apply the load until failure. The loading speed varied based on the CLT layup, with each test lasting approximately 5 min until failure.

To measure deflection during loading, a displacement transducer (SDP-200D, Tokyo Measuring Instruments Laboratory Co., Ltd.) was brought into contact with an L-shaped bracket, which was attached to the mid-span and mid-depth of the specimen's side face. In addition, a yoke with a displacement transducer (CDP-10, Tokyo Measuring Instruments Laboratory Co., Ltd.) was positioned on the top surface of the specimen to measure deflection between the loading points.

Using these measurements, both the global (apparent) and local (true or shear-free) bending moduli of elasticity were calculated. The global modulus was derived from the total deflection under load, whereas the local modulus was obtained from the deflection measured between the loading points.

To determine moisture content using the oven-dry method, a small sample (approximately 30 mm in length) was cut near the failure location of each specimen after the bending test. The methods for measuring the modulus of elasticity and G are summarized in Table 2.

In addition to the tests on CLT specimens, longitudinal vibration and bending tests were performed on the laminae. During the longitudinal vibration tests, each lamina specimen was supported at its mid-length. Longitudinal vibrations were induced by striking one cross-sectional end with a hammer and subsequently detected by a microphone placed at the opposite end. The first resonant frequency was then recorded using an FFT analyzer (CF-4500, Ono Sokki Co., Ltd.).

For the laminae bending tests, which conformed to JAS 3079 [10], bending test C, a third-point loading configuration was used with the span set at 21 times the specimen depth. Load was applied at 10 mm/min until failure by a universal testing machine (TCM 10000, MinebeaMitsumi Inc.). To measure deflection during loading, a displacement transducer (CDP-50, Tokyo Measuring Instruments Laboratory Co., Ltd.) was brought into contact with an L-shaped bracket, which was attached to the mid-span and mid-depth of the specimen's side face. These measurements were then used to calculate the global E_{app}.

Results and discussion

Comparison of modulus of elasticity and shear modulus by each method

The E and G results from dynamic, static, and bending tests are summarized in Table 3. Figures 4, 5 and 6 show the mean values of E, G, and their ratio (E/G) for each of these test methods.

The modulus of elasticity calculated using the E_{TS} [12, 20] is given by the following equations:

$$E_{TS} = E_{b_oml} \times \frac{I_A}{I_0} \tag{1}$$

$$I_A = \frac{\Sigma\left(E_i I_i + E_i A_i z_i^2\right)}{E_0} \tag{2}$$

where:

E_{b_oml} = the bending modulus of elasticity of the lamina, specifically the one in the outermost layer (for major strength direction evaluation), or the outermost lamina in the inner layer (for minor strength direction evaluation).

Table 2 Summary of methods used to measure the modulus of elasticity and shear modulus

Property	Test type	Method	Symbol
Modulus of elasticity	Dynamic test	Longitudinal vibration	E_{fr}
		Timoshenko–Goens–Hearmon (TGH)	E_{TGH}
	Static test	Variable span, Three-point bending	E_{VS}
		Global (apparent), Third-point bending	E_{glo}
		Local (shear-free), Third-point bending	E_{loc}
Shear modulus	Dynamic test	Timoshenko–Goens–Hearmon (TGH)	G_{TGH}
	Static test	Variable span, Three-point bending	G_{VS}

Table 3 Summary of modulus of elasticity and shear modulus obtained from dynamic, static, and bending tests

Group	E_{fr} (kN/mm^2)	E_{TGH} (kN/mm^2)	E_{VS} (kN/mm^2)	E_{glo} (kN/mm^2)	E_{loc} (kN/mm^2)	G_{TGH} (kN/mm^2)	G_{VS} (kN/mm^2)
9L9P-Ma	4.45 (3.46)	6.13 (3.29)	5.84 (3.10)	5.39 (4.51)	6.06 (4.96)	0.243 (4.18)	0.186 (6.82)
9L9P-Mi	3.23 (2.31)	2.53 (3.62)	2.40 (3.53)	2.32 (3.28)	2.49 (6.06)	0.212 (2.76)	0.139 (9.15)
7L7P-Ma	4.50 (3.10)	6.55 (3.77)	6.36 (6.21)	5.92 (6.32)	6.77 (7.39)	0.248 (8.14)	0.198 (13.58)
7L7P-Mi	2.55 (3.36)	1.85 (1.69)	1.74 (3.75)	1.67 (8.54)	1.83 (10.09)	0.158 (2.29)	0.103 (29.34)
5L7P-Ma	6.08 (2.97)	8.22 (3.81)	8.15 (4.25)	7.43 (4.33)	8.52 (5.07)	0.304 (2.72)	0.171 (8.08)
5L7P-Mi	1.89 (4.53)	0.84 (3.32)	0.72 (6.75)	0.70 (5.24)	0.72 (5.19)	0.130 (7.94)	0.057 (35.23)
5L5P-Ma	4.96 (7.84)	7.25 (8.87)	7.12 (8.78)	6.77 (7.73)	7.60 (8.93)	0.254 (2.84)	0.174 (6.45)
5L5P-Mi	2.47 (4.48)	1.49 (2.93)	1.43 (7.94)	1.41 (5.48)	1.47 (4.50)	0.150 (1.03)	0.084 (22.41)
3L4P-Ma	5.01 (3.03)	7.86 (2.52)	8.30 (2.24)	7.06 (2.65)	8.68 (3.20)	0.149 (5.91)	0.105 (5.56)
3L4P-Mi	2.97 (4.53)	1.07 (3.10)	1.12 (7.26)	0.96 (3.94)	1.00 (5.72)	0.416 (4.46)	0.089 (28.53)
3L3P-Ma	6.38 (6.48)	8.90 (6.74)	8.73 (8.06)	8.12 (6.07)	9.52 (9.08)	0.249 (6.22)	0.138 (8.14)
3L3P-Mi	1.97 (6.89)	0.53 (5.58)	0.44 (3.58)	0.47 (6.58)	0.45 (9.70)	0.336 (24.60)	0.069 (21.78)

Values on the left represent the means, while those in parentheses on the right indicate the coefficients of variation (%). For symbol definitions, see Table 2

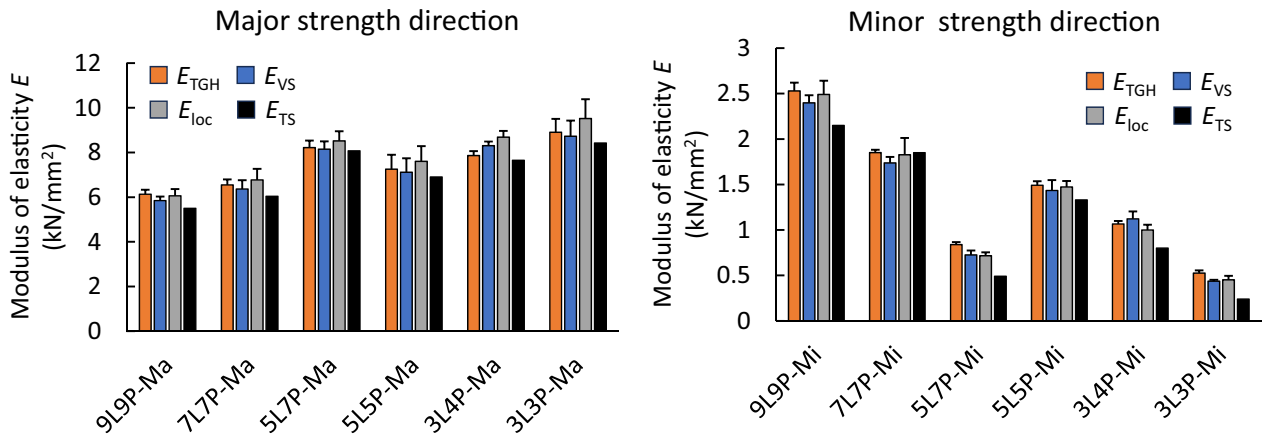


Fig. 4 Mean values of the modulus of elasticity (*E*). Error bars represent standard deviations. E_{TS} refers to the modulus of elasticity calculated by the transformed section method. For other symbols, refer to Table 2.

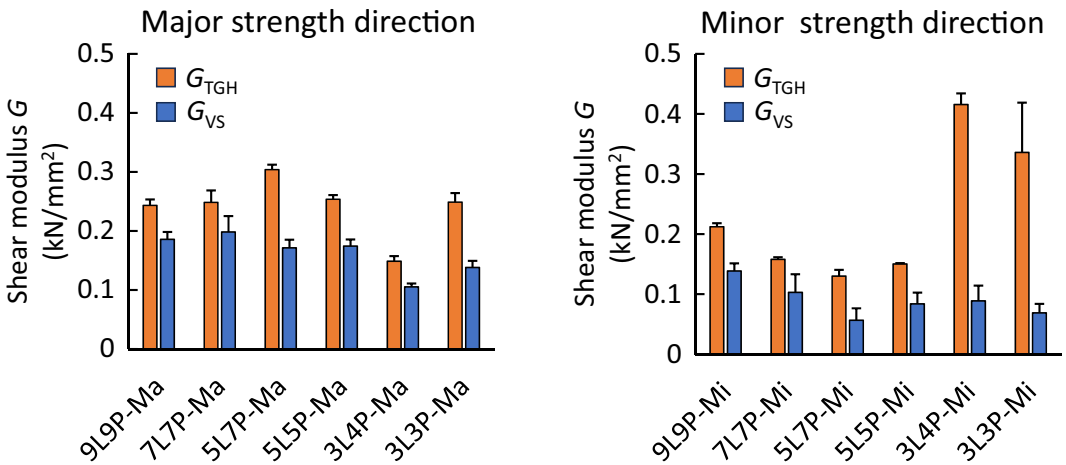


Fig. 5 Mean values of the shear modulus (*G*). Note: Error bars represent standard deviations. For symbol definitions, see Table 2.

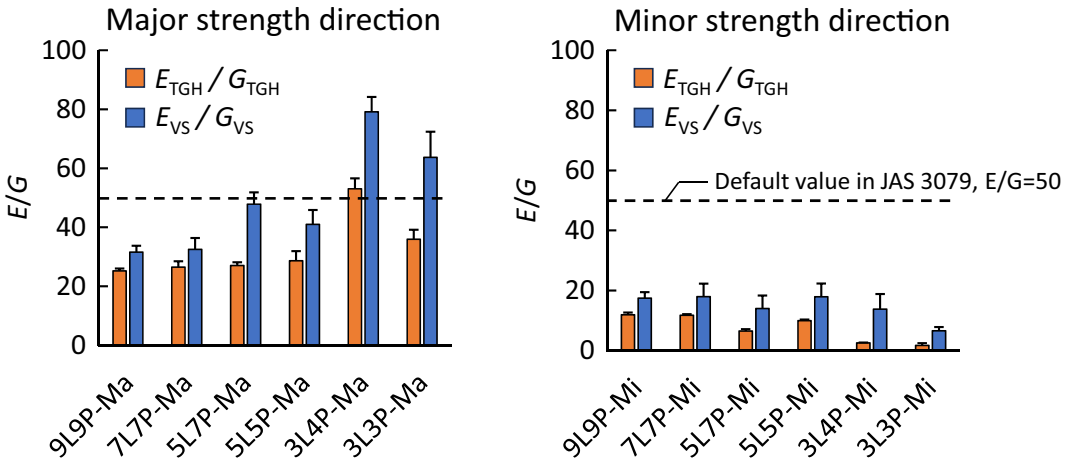


Fig. 6 Ratio of modulus of elasticity to shear modulus (*E*/*G*). Error bars represent standard deviations.

I_A = the second moment of area of the transformed section of the CLT.

I_0 = the second moment of area of the CLT.

E_i = the bending modulus of elasticity of the lamina used in the *i*th layer; for laminae oriented perpendicular to the specimen length, the modulus is taken as zero.

I_i = the second moment of area of the *i*th layer.

A_i = the cross-sectional area of the *i*th layer.

z_i = the distance between the neutral axis of the CLT and the centroid of the lamina in the *i*th layer.

E_0 = same as E_{b_oml}.

The values of E_{b_oml} and E_0 used in the E_{TS} were determined as the mean modulus of elasticity obtained from longitudinal vibration measurements: 8.74 kN/mm^2 for M60B layers aligned parallel to the specimen length, and 6.41 kN/mm^2 for M30B layers aligned parallel to the specimen length. Layers perpendicular to the specimen length had their modulus of elasticity set to 0 kN/mm^2.

Figure 4 shows the modulus of elasticity obtained by each method. No considerable difference was observed between the values from the TGH method (E_{TGH}), the variable span method (E_{VS}), and the local method (E_{loc}). However, the values calculated using the E_{TS} tended to be lower than those from the other methods, except in a few layups. One possible reason is that assigning a modulus of elasticity of 0 kN/mm^2 to the cross layers in the E_{TS} was inappropriate. For example, the CLT Handbook [1] sets the modulus of elasticity of the cross layers at 1/30 that of the parallel layers. Based on this, an additional calculation using the E_{TS} was performed with this assumption. The results showed almost no change in E_{TS} values in the major strength direction. However, in the minor strength direction, the E_{TS} values increased by factors of 1.08, 1.11, 1.53, 1.17, 1.33, and 2.17 for the 9L9P-Mi, 7L7P-Mi, 5L7P-Mi, 5L5P-Mi, 3L4P-Mi, and 3L3P-Mi layups, respectively.

The mean G obtained by the TGH method (G_{TGH}) was consistently higher than that from the variable span method (G_{VS}) across all layups, as shown in Fig. 5. This difference was particularly notable in the minor strength direction, specifically for the 3L4P-Mi and 3L3P-Mi layups, where G_{TGH} greatly surpassed G_{VS}.

To investigate this discrepancy, Fig. 7 shows the typical relationship between $(d/L)^2$ and $1/E_{app}$, which forms the basis for calculating E_{vs} and G_{vs} according to Timoshenko's beam theory. While this relationship is theoretically expected to show a monotonic increase owing to shear deformation, and most major strength direction specimens followed this trend, Fig. 7 numerically demonstrates that for 3L3P-Mi, 3L4P-Mi, and especially the excluded specimens, some plots exhibited a decrease in $1/E_{app}$ despite an increase in $(d/L)^2$.

Whether this reverse trend was owing to simple measurement error or some intrinsic properties of the minor strength direction specimens is still unclear. Should the deformation measurements be accurate, the variable span method may prove unsuitable for CLT specimens with minor strength direction layups.

As shown in Fig. 6, the E/G ratio from the variable span method was consistently higher than that from the TGH method for all layups. Moreover, in both methodologies, specimens in the major strength direction consistently presented higher E/G ratios compared to those in the minor strength direction. Remarkably, three major strength direction layups—3L4P-Ma (TGH method), 3L4P-Ma (variable span method), and 3L3P-Ma (variable span method)—exceeded the JAS 3079 [10] default E/G ratio of 50. The highest recorded

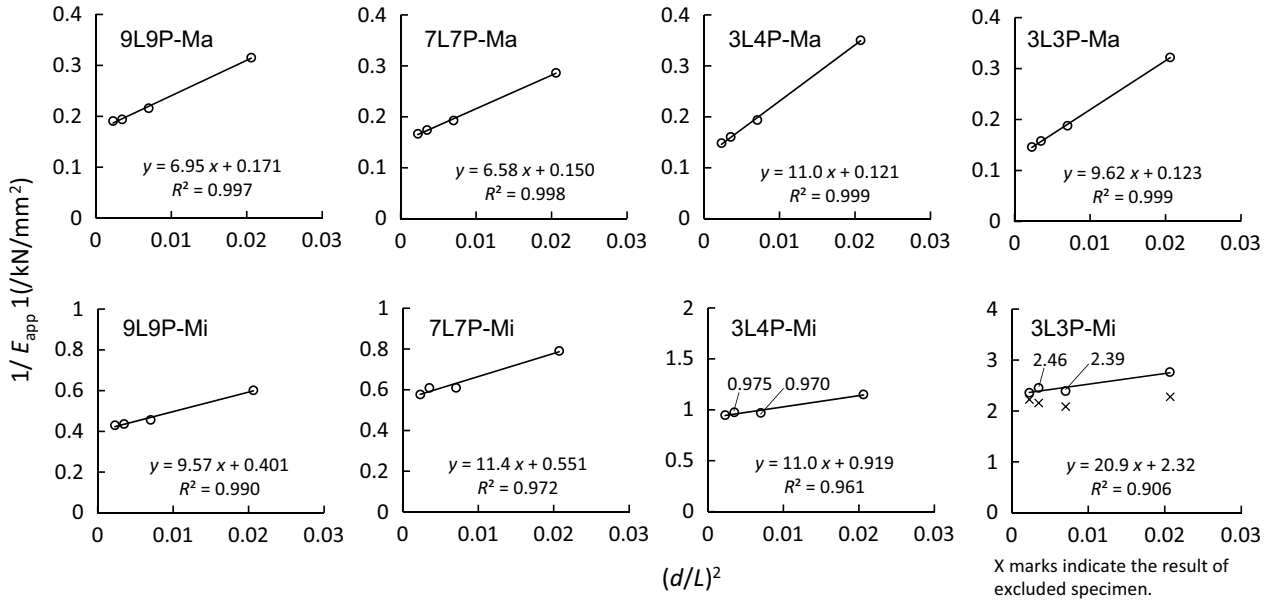


Fig. 7 Typical relationship between $(d/L)^2$ and $1/E_{app.}$ d is the specimen depth, L is the span, and E_{app} is the apparent bending modulus of elasticity.

E/G ratio, approximately 80, was obtained for the 3L4P-Ma layup using the variable span method.

In stark contrast, the TGH method yielded an E/G ratio below 2 for 3L3P-Mi, a value lower than the theoretical minimum for isotropic materials. This anomaly strongly suggests that the assumption of homogeneity, fundamental to estimating equivalent modulus of elasticity and G values, may be invalid for certain layups, including 3L3P-Mi. As a result, test methods derived from classical beam theory may be unsuitable for evaluating CLT in the minor strength direction, especially for layups such as 3L3P-Mi. A more comprehensive investigation into this issue is, therefore, necessary.

To investigate the E when the E/G ratio exceeds 80, Eq. (4) was used. Adapted from ASTM D2915 [21] Eq. (3), this equation allows for the conversion of the E_{true} to the apparent bending modulus under third-point loading ($L/d=21$), a configuration aligned with JAS 3079 [10]. The ratio between the true and apparent bending moduli was then calculated using this equation for an E/G value of 80:

$$E_2 = \frac{1 + K_1\left(\frac{d_1}{L_1}\right)\left(\frac{E}{G}\right)}{1 + K_2\left(\frac{d_2}{L_2}\right)\left(\frac{E}{G}\right)} E_1 \tag{3}$$

$$E_{app}/E_{true} = \frac{1}{1 + \left(\frac{216}{230}\right)\left(\frac{d}{L}\right)\left(\frac{E}{G}\right)} \tag{4}$$

where:

E_1, d_1, L_1 = apparent bending modulus of elasticity, depth, and span at test condition 1.

E_2, d_2, L_2 = apparent bending modulus of elasticity, depth, and span at test condition 2.

K_1, K_2 = values given in ASTM D2915 Table X4.1

By substituting $d/L=1/21$ and $E/G=80$ into Eq. (4), the ratio of the E_{true} to the E_{app} is calculated as 0.85. Figure 8 shows the relationship between the span-to-depth ratio (L/d) and the apparent-to-true bending modulus ratio, as derived from Eq. (4), for E/G values of 80 and 50. The ratio of the apparent-to-true adjustment factor at

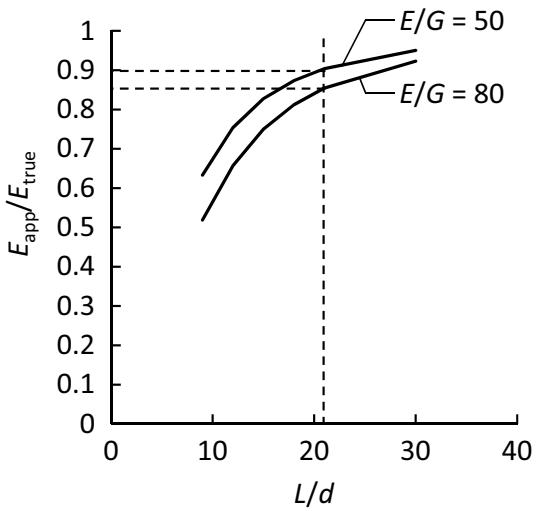


Fig. 8 Span-to-depth ratio versus apparent-to-true bending modulus of elasticity ratio (E_{app}/E_{true})

$E/G = 50$ (the JAS 3079 [10] default) to that at $E/G = 80$ is $0.85/0.90 = 0.94$. This means that the E_{app} for CLT with an E/G of 80 is approximately 94% of the value based on the JAS 3079 [10] default E/G of 50. The current adjustment factor based on JAS 3079 [10] should generally not pose considerable issues for typical CLT manufacturing. However, for layups, such as 3L4P Ma and 3L3P Ma, which are highly susceptible to rolling shear, the use of laminae with a modulus of elasticity close to the lower limit could result in a measured CLT E that is slightly lower than the value specified in JAS 3079 [10].

Results of out-of-plane bending test

Figure 9 depicts typical failure modes for several layups, complementing the out-of-plane bending test results summarized in Table 4. While most major strength direction specimens failed at finger joints or knots on the tensile side, the 3L4P-Ma layup stood out with all specimens failing in shear. Regardless of shear failure, the strength for these cases was still calculated as bending strength from the maximum load. In contrast, in the minor strength direction, failure consistently initiated above the points, where the outer laminae were

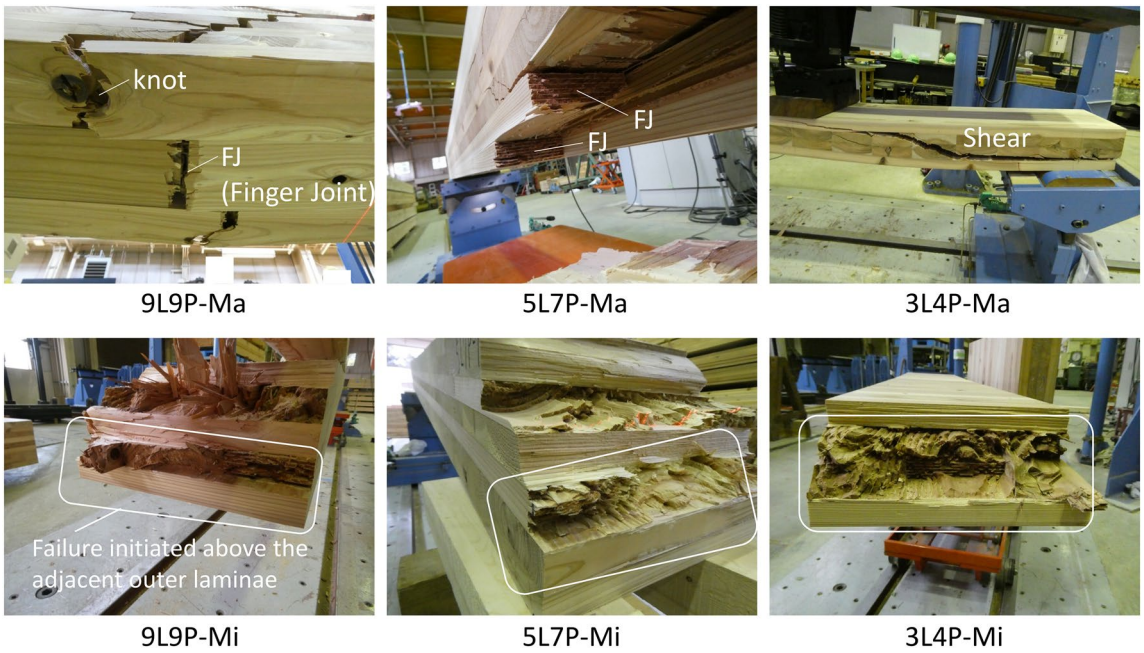


Fig. 9 Typical failure modes for various layups

Table 4 Summary of out-of-plane bending test results

Group	Density (kg/m^3)	MC (%)	σ_b (N/mm^2)	Failure mode and number
9L9P-Ma	383 (0.70)	10.6 (3.5)	18.6 (7.3)	Bending: 8
9L9P-Mi	382 (1.06)	10.0 (6.6)	10.3 (10.8)	Bending: 8
7L7P-Ma	382 (1.39)	10.7 (4.8)	21.0 (14.0)	Bending: 8
7L7P-Mi	387 (1.25)	10.1 (2.5)	9.3 (12.1)	Bending: 8
5L7P-Ma	391 (2.56)	10.6 (5.8)	28.9 (9.0)	Bending: 7, Bending + Shear: 1
5L7P-Mi	385 (1.45)	10.6 (4.4)	4.8 (11.7)	Bending: 8
5L5P-Ma	394 (0.67)	9.4 (3.8)	26.9 (13.9)	Bending: 6
5L5P-Mi	381 (0.71)	9.7 (3.6)	9.1 (11.4)	Bending: 6
3L4P-Ma	408 (1.44)	8.0 (1.6)	25.2 (3.0)	Shear: 6
3L4P-Mi	390 (1.84)	10.6 (5.2)	7.0 (8.5)	Bending: 6
3L3P-Ma	398 (2.71)	10.7 (5.2)	30.7 (16.5)	Bending: 6
3L3P-Mi	401 (4.18)	10.4 (4.4)	4.4 (8.9)	Bending: 6

Values on the left are means, and values in parentheses on the right represent coefficients of variation (%). MC: Moisture content, σ_b: Bending strength

laterally adjacent, and all specimens exhibited bending failure.

Below, we present the mean measured bending strength for each CLT layup, alongside the estimated bending strength ($\sigma_{\text{b-est}}$), which was calculated using E_{TS} as described in the Notification of the Ministry of Land, Infrastructure, Transport and Tourism [12, 20]

$$\sigma_{\text{b-est}} = \sigma_{\text{b_oml}} \times \frac{I_{\text{A}}}{I_0} \tag{5}$$

where:

$\sigma_{\text{b-oml}}$ = the bending strength of the lamina, referring to either the outermost layer's lamina (for major strength direction evaluation) or the outermost lamina in the inner layer (for minor strength direction evaluation).

As previously outlined, the modulus of elasticity was used for estimating bending strength. For $\sigma_{\text{b-oml}}$, its value was determined based on the loading direction. In the major strength direction, the bending strength of the outermost layer was assigned 37.4 N/mm^2 (the mean value of the M60B lamina). Conversely, when evaluating the minor strength direction, the outer perpendicular layer was considered ineffective, and the relevant bending strength for $\sigma_{\text{b-oml}}$ was 28.6 N/mm^2 (the mean M30B lamina value), applied to the outermost parallel layer in the inner part of the specimen.

Figure 10 shows the relationship between measured and estimated bending strength values. The blue bars represent estimated values based on the lamina's bending strength (details on green bars are provided in the next paragraph). A clear trend emerged in the major strength direction: estimated values consistently exceeded measured mean values for all layups. In contrast, in the minor strength direction, the measured mean values surpassed the estimated values for every layup, although the difference was somewhat less pronounced for the 9L9P-Mi and 7L7P-Mi layups.

Although the bending strength of CLT in this study was estimated based on the lamina's bending strength, it may be more appropriate in some instances to use the tensile strength parallel to the grain instead, because failure frequently originates from the tensile layer.

The authors' previous study [22] involved performing bending and parallel-to-grain tensile tests on two grades of Japanese cedar laminae: M60A (characterized by an E of at least 5.0 kN/mm^2) and M30A (an E of at least 2.5 kN/mm^2). Each specimen contained a single finger joint at the center. The results indicated that the ratio of tensile strength to bending strength was 0.70 for M60A and 0.65 for M30A.

The tensile strengths of M60B and M30B laminae were estimated to be 26.2 and 18.6 kN/mm^2, respectively, using the abovementioned ratios. Figure 10's green bars show the resulting estimated CLT bending strength, which is based on the lamina's tensile strength. In the major strength direction, the measured values consistently surpassed these estimates,

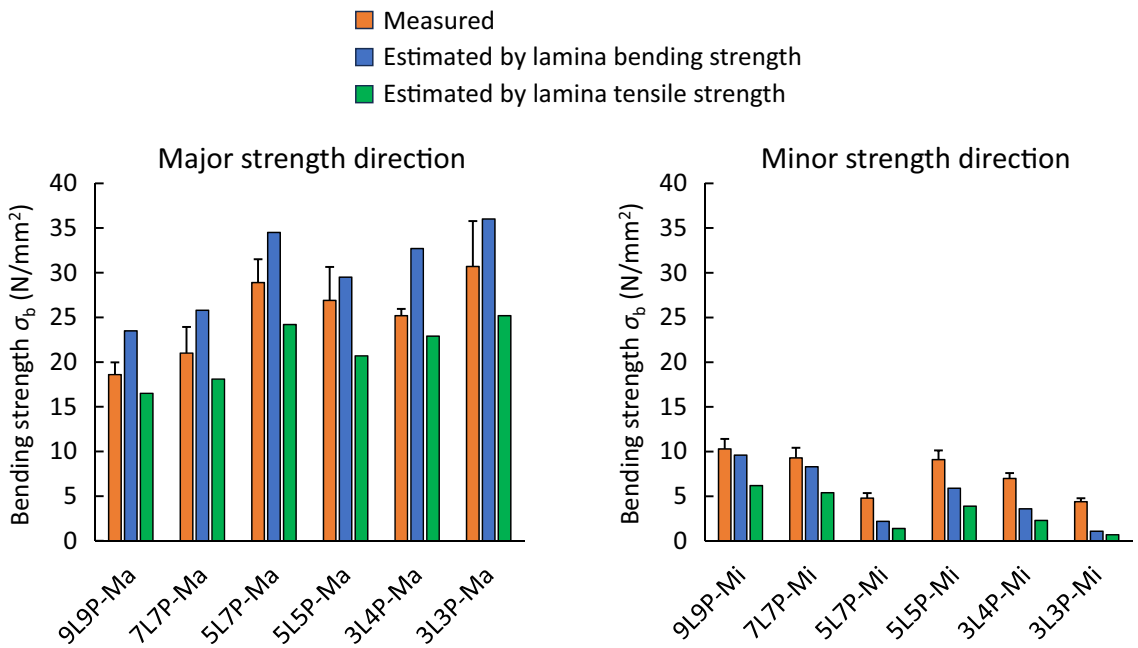


Fig. 10 Measured versus estimated bending strength using the transformed section method from the notification [20]. Note: Error bars represent standard deviations

yielding measured-to-estimated ratios between 1.10 and 1.30, dependent on the specific layup.

For the minor strength direction, estimates based on tensile strength produced even lower predicted values. However, even when bending strength was used, the measured values still exceeded the estimates in this direction. This discrepancy suggests that the bottom outer lamina in minor strength direction specimens, being unbonded in the width direction, may not contribute structurally. Therefore, the CLT's overall strength in this orientation appears to depend mainly on the second layer from the bottom.

Despite the expectation that failure would typically initiate at the weakest part of the second layer, the outer lamina might provide reinforcement through lamination bonding. As depicted in Fig. 9, minor strength direction failure consistently initiated above the points, where the outer laminae were laterally adjacent. Among the three laminae in the second layer's width, some displayed failure at typical weak points, such as finger joints and knots, while others did not. This localized failure pattern strongly suggests a reinforcing effect provided by the outer layer.

For the major strength direction, the North American CLT standard applies a 0.85 adjustment factor to the calculated bending moment resistance of CLT panels. This factor is based on comparisons between full-scale bending test results and shear analogy model calculations for panels with seven or more layers [23–25]. Importantly, this 0.85 adjustment factor is not applied in the minor strength direction. However, a separate 0.9 resistance factor is applied in both the major and minor strength directions.

In Japan, based on these findings, an adjustment factor of 0.65 is applied to the calculation results obtained using the transformed section method for both the major and minor strength directions [20]. Furthermore, to calculate the specified design strength (i.e., the lower limit), an additional 0.75 adjustment factor is incorporated, which considers the coefficient of variation in out-of-plane bending strength [20].

In the major strength direction, estimates based on the lamina's bending strength surpassed the measured mean values (Fig. 10). Therefore, the application of the 0.65 adjustment factor seems appropriate. Conversely, applying this same adjustment factor in the minor strength direction may be overly conservative, particularly because North American standards do not apply their 0.85 adjustment factor in that specific direction.

Conclusions

This study investigated the out-of-plane bending performance of Japanese cedar CLTs, including the evaluation of their modulus of elasticity and G using dynamic and static test methods. Six CLT layups, as specified in JAS 3079 [10], were compared across both major and minor strength directions. The following conclusions were made.

1. The modulus of elasticity values obtained from the TGH method, the variable span method, and the local method in bending tests were generally consistent, whereas those calculated using the E_{TS} tended to be lower, especially for layups in the minor strength direction.
2. The G values derived from the TGH method consistently surpassed those obtained from the variable span method, a difference especially pronounced in minor strength direction layups, such as 3L3P-Mi and 3L4P-Mi. Furthermore, the variable span method exhibited irregular trends in certain specimens, indicating its potential unsuitability for CLT configurations featuring fewer layers in the minor strength direction.
3. E/G ratios from the variable span method were consistently higher than those from the TGH method. Notably, certain major strength direction layups, including 3L4P-Ma and 3L3P-Ma, exceeded the JAS 3079 [10] default E/G ratio of 50, reaching values up to 80, which corresponds to an adjustment factor of approximately 0.85. While the JAS 3079's 0.9 adjustment factor is suitable for most practical CLT layups, it may underestimate deformation in rolling shear-prone configurations, such as 3L4P-Ma and 3L3P-Ma.
4. The out-of-plane bending test results suggest that the application of a 0.65 adjustment factor is reasonable for the major strength direction, because estimated values consistently surpassed measured ones. Conversely, applying this same factor in the minor strength direction appears to be excessively conservative.

Abbreviations

JAS	Japanese agricultural standard
CLT	Cross-laminated timber
API	Aqueous polymer-isocyanate
FFT	Fast Fourier transform
TGH	Timoshenko–Goens–Hearmon
MC	Moisture content

Acknowledgements

The authors would like to thank Mr. Genji Kojima of Gunma Prefectural Forestry Experiment Station for his assistance with the testing. This study's

findings were partly presented at the 75th annual meeting of the Japan Wood Research Society in March 2025.

Author contributions
HI designed the study, conducted the experiments, analyzed the data, and is the primary contributor to writing the manuscript. RS conducted the experiments, contributed to the data analysis, and participated in manuscript writing. KM contributed to the study design and prepared the test specimens. AM contributed to the study design and data analysis. All authors have read and approved the final manuscript.

Funding
This study was subsidized by the Forestry Agency in 2023 under the "Subsidy for comprehensive measures for green growth of forest, forestry, and lumber industries" program.

Data availability
The data sets analyzed during this study are available from the corresponding author upon reasonable request.

Declarations

Ethics approval and consent to participate
Not applicable.

Consent for publication
Not applicable.

Competing interests
The authors declare no competing interests.

Received: 16 May 2025 Accepted: 17 August 2025
Published: 28 August 2025

References

1. FPInnovations (2011) Chapter 3 Structural design of cross-laminated timber elements. In: CLT Handbook: cross-laminated timber Canadian edition. FPInnovations, Quebec, pp 1–63
2. Okabe M, Yasumura M, Kobayashi K, Fujita K (2013) Prediction of bending stiffness and moment carrying capacity of sugi cross-laminated timber. J Wood Sci 60:49–58
3. Christovasilis IP, Brunetti M, Follesa M, Nocetti M, Vassallo D (2016) Evaluation of the mechanical properties of cross laminated timber with elementary beam theories. Constr Build Mater 122:202–213
4. Niederwestberg J, Zhou J, Chui YH (2018) Comparison of theoretical and laboratory out-of-plane shear stiffness values of cross laminated timber panels. Buildings 8:146
5. Sandoli A, Calderoni B (2020) The rolling shear influence on the out-of-plane behavior of CLT panels: a comparative analysis. Buildings 10:42
6. Rahman MDT, Ashraf M, Ghabraie K, Subhani M (2020) Evaluating Timoshenko method for analyzing CLT under out-of-plane loading. Buildings 10:184
7. Olsson A, Schirén W, Segerholm K, Bader TK (2023) Relationship between stiffness of material, lamellas and CLT elements with respect to out of plane bending and rolling shear. Eur J Wood Wood Prod 81:871–886
8. Huang Z, Jiang L, Ni C, Chen Z (2023) The appropriacy of the analytical models for calculating the shear capacity of cross-laminated timber (CLT) under out-of-plane bending. J Wood Sci 69:14
9. Huang Z, Bian Y, Ni C (2024) A rolling shear analysis-based method for determining the apparent stiffness and bending capacity of CLT panel under out-of-plane load. J Wood Sci 70:8
10. Notification No. 3079 of the Ministry of Agriculture, Forestry and Fisheries, February 28 (2025) Japanese Agricultural Standard for Cross Laminated Timber, Ministry of Agriculture, Forestry and Fisheries, Tokyo (in Japanese).
11. Timoshenko S (1958) Strength of materials. Part I elementary theory and problems. Van Nostrand Reinhold Company, New York, pp 217–221
12. CLT Design and Construction Manual Editorial Committee (2024) Design and construction manual for buildings using CLT. Japan Housing and Wood Technology Center. Tokyo, pp 293–322 (in Japanese).
13. Ido H, Nagao H, Harada M, Kato H, Ogiso J, Miyatake A (2016) Effects of the width and lay-up of sugi cross-laminated timber (CLT) on its dynamic and static elastic moduli, and tensile strength. J Wood Sci 62:101–108
14. Forestry and Forest Products Research Institute, Hokkaido Forest Products Research Institute, Japan CLT Association (2015) Report on the promotion of practical use of CLT (collection and analysis of strength data). (in Japanese) https://www.ffpri.affrc.go.jp/pubs/various/documents/h25clttkyoudo.pdf. Accessed 17 April 2025.
15. Komatsu K, Nakatani M, Nakahara T, Komatsu K, Noda Y (2021) Mechanical performances of finger jointed cross laminated timber (CLT). Eur J Wood Prod 79:397–416
16. Yamamoto K, Fujita K, Watanabe Y, Miyatake A, Shibusawa T, Tanaka S, Kanayama K (2021) Flexural property in out-of-plane bending test of cross laminated timber (CLT) composed of different grade lamina of sugi. J Soc Mater Sci Jpn 70:561–566
17. Kubojima Y, Yoshihara H, Ohta M, Okano T (1996) Examination of the method of measuring the shear modulus of wood based on the Timoshenko theory of bending. Mokuzai Gakkaishi 42:1170–1176
18. Kubojima Y, Tonosaki M (2012) Young's and shear moduli of glued laminated timber composed of different species obtained by a flexural vibration test. Holzforschung 66:871–875
19. ASTM D198-22 (2022) Standard test methods of static tests of lumber in structural sizes. ASTM International, West Conshohocken, vol 04–10.
20. Notification No. 1024 of the Ministry of Land, Infrastructure, Transport and Tourism, June 12 (2001) Establishment of special allowable unit stress and special material strength. Ministry of Land, Infrastructure, Transport and Tourism, Tokyo (in Japanese).
21. ASTM D2915-17 (2022) Standard practice for sampling and data-analysis for structural wood and wood-based products. ASTM International, West Conshohocken, vol 04–10.
22. Japan Wood Preserves Industry Association (2022) Report on data collection and research project for the standardization of preservative-treated cross-laminated timber (CLT) under Japanese agricultural standards. (in Japanese) http://www.jwpia.or.jp/pages/1/detail=1/b_id=3/r_id=18/ Accessed 17 April 2025.
23. ANSI/APA PRG 320 (2018) Standard for performance-rated cross-laminated timber. APA – The Engineered Wood Association, Tacoma, Washington.
24. Yeh B, Gagnon S, Williamson T, Pirvu C (2012) The cross-laminated timber standard in north America. In: Proceedings of the World Conference on Timber Engineering. July 15–19, 2012, Auckland, New Zealand.
25. CSA O86:24 (2024) Engineering design in wood. CSA Group, Canadian Standard Association, Mississauga, Ontario.

Publisher's Note

Springer Nature remains neutral with regard to jurisdictional claims in published maps and institutional affiliations.